

VUV LASER DIAGNOSTICS OF H⁺ ION SOURCES**A.T. Young, G.C. Stutzin, K.N. Leung, and W.B. Kunkel**

**Accelerator and Fusion Research Division
Lawrence Berkeley Laboratory
University of California
1 Cyclotron Road
Berkeley, California 94720**

DISCLAIMER

This report was prepared as an account of work sponsored by an agency of the United States Government. Neither the United States Government nor any agency thereof, nor any of their employees, makes any warranty, express or implied, or assumes any legal liability or responsibility for the accuracy, completeness, or usefulness of any information, apparatus, product, or process disclosed, or represents that its use would not infringe privately owned rights. Reference herein to any specific commercial product, process, or service by trade name, trademark, manufacturer, or otherwise does not necessarily constitute or imply its endorsement, recommendation, or favoring by the United States Government or any agency thereof. The views and opinions of authors expressed herein do not necessarily state or reflect those of the United States Government or any agency thereof.

This work has been supported by the Air Force Office of Scientific Research, Los Alamos National Laboratory, and the Director, Office of Energy Research, Office of Fusion Energy, Development and Technology Division, of the U.S. Department of Energy under contract No. DE-AC03-76SF00098.

MASTER

ep

VUV LASER DIAGNOSTICS OF H⁻ ION SOURCES

A.T. Young, G.C. Stutzin, K.N. Leung, and W.B. Kunkel
Lawrence Berkeley Laboratory, University of California,
Berkeley, California 94720

ABSTRACT

Vacuum ultraviolet laser absorption spectroscopy has been employed to measure the populations and temperatures of ground electronic state H-atoms and vibrationally-excited H₂ molecules in a volume H⁻ ion source. Measurements of both species have been made under a variety of discharge conditions. Vibrational levels to v⁻=8 have been measured, with the vibrational population distribution well described by a temperature of 4150K.

INTRODUCTION

Ground-electronic state atomic hydrogen, H⁰, and vibrationally-excited hydrogen molecules, H₂(v^{*}), are thought to play crucial roles in the generation of H⁻ in multicusp volume sources. In these sources, H₂(v^{*}) is thought to form H⁻ via collisions with low-energy electrons (dissociative attachment), while H⁻ can be destroyed by H⁰ in the reverse reaction. In order to further the understanding of the physical and chemical processes occurring in these sources, accurate determinations of the density, translational temperature, and state distribution of these species are required. For this reason, vacuum ultraviolet (VUV) laser absorption spectroscopy has been developed to measure these species. This technique allows for the direct, sensitive, and state-specific detection of the ground electronic state H⁰ and H₂(v^{*}), requiring no assumptions about plasma parameters such as the electron density distribution. The measurement is performed "in-situ," in a non-perturbative fashion. The technique gives the average density of the absorbing species along the absorption path, providing a direct measure of the species within the discharge volume.

In this paper, some of the recent measurements of H⁰ and H₂(v^{*}) using VUV laser absorption spectroscopy are reviewed. These data, obtained on a prototypical multicusp H⁻ source, cover a variety of discharge conditions and will help lead to an increased understanding of the H⁻ production mechanisms in these sources.

EXPERIMENTAL

H⁰ and H₂(v^{*}) are detected using VUV laser absorption spectroscopy. The experimental apparatus has been described in detail previously,¹ and is shown schematically in Figure 1. Briefly, frequency-tunable 20 ns pulses of VUV are produced by the non-linear optical technique of four-wave sum frequency mixing. For the particular wavelengths of interest, mercury vapor is used as the mixing medium. By using various resonance levels in the mercury, efficient generation of light from 94 to 125 nm has been accomplished. After generation, a portion of the VUV is measured and used for normalization, while the majority of the VUV, the "probe beam," is directed to the plasma chamber where absorption by H⁰ or H₂(v^{*}) occurs. The measured absorbance $a(\lambda) \equiv \ln[I_{off}(\lambda)/I_{on}(\lambda)]$ is then plotted as a function of VUV wavelength to obtain the absorption spectrum. Here $I(\lambda)$ is the intensity of the normalized probe beam after passage through the plasma chamber and the subscripts refer to the discharge off or on. The narrow bandwidth of the VUV,

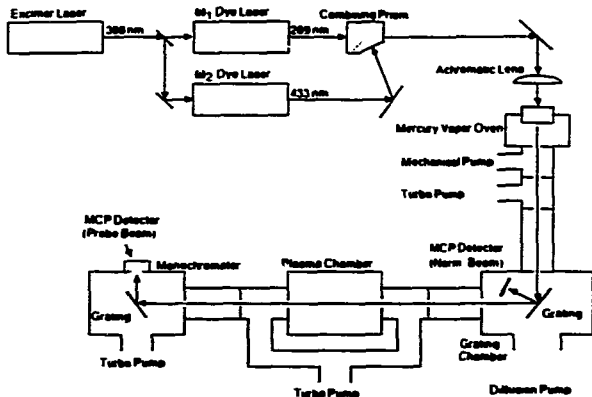


Figure 1. Schematic diagram of VUV absorption spectrometer system. Wavelengths shown are for generation of Lyman- β radiation.

-0.3 cm^{-1} ($\approx 3 \times 10^{-4} \text{ nm}$), makes possible the determination of the lineshape of the absorption feature. The total area under the absorption profile is proportional to the density of the absorbing species. The width of the line, assumed to be due to Doppler broadening, gives the translational temperature of the species.

The plasma chamber used for these experiments is a water cooled stainless steel multicusp source, 230 mm long and 200 mm in diameter. Ten rows of permanent magnets along the cylinder walls formed the cusped field. The end flanges of the source are also equipped with magnets. A coaxial LaB_6 cathode, 6 mm diameter \times 10 mm long, was mounted on a holder of tungsten and tantalum and used as a thermionic electron source in these experiments. The absorption path was longitudinal through the source and slightly offset from, but parallel to, the cylinder axis. Differential pumping apertures defined the pathlength: which was measured to be 31 cm. Hydrogen pressures, p_{H_2} , reported here are measured with a capacitance manometer with the discharge off.

Atomic density measurements were obtained using the Lyman β , Lyman γ , or Lyman ϵ ($n=3 - n=1$, $n=4 - n=1$, and $n=6 - n=1$) transitions of H^* at 102.6 nm, 97.3 nm and 93.8 nm, respectively. Individual rotation-vibrational states of $\text{H}_2(v^*)$ were measured using the B - X (Lyman) or C - X (Werner) bands.^{3,4} These lines occur from 110 nm to 126 nm.

RESULTS

A typical absorption spectrum of H^* is shown in Figure 2. This spectrum was obtained with the Lyman- γ transition and discharge parameters of 25 A, 150 V at a pressure of 7mTorr. The line through the experimental data points is a least squares fit of the data by the sum of two Gaussians having a common central wavelength but different widths. Such a lineshape is characteristic of a population with a bimodal velocity distribution. The data is consistent with 60% of the atoms characterized by $T_{\text{trans}} = 700 \text{ K}$ and 40% of the atoms at $T_{\text{trans}} = 7300 \text{ K}$. The total H^* density, $9.4 \times 10^{12} \text{ cm}^{-3}$, represents 2% of the H_2 initially in the source being dissociated.

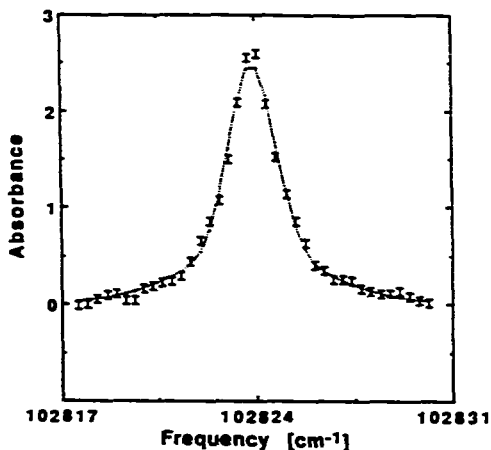


Figure 2. Typical H^+ absorption spectrum. This spectrum obtained using Lyman- γ Discharge conditions are 25A, 150V, and $p_{H_2} = 7$ mTorr. $[H^+] = 9.4 \times 10^{12}$ atoms- cm^{-3} .

The H^+ density was measured as a function of various discharge parameters, including discharge voltage and current, and H_2 pressure. Figure 3 displays the H^+ density as a function of H_2 pressure. As can be seen, the H^+ density rises approximately linearly with H_2 pressure, and represents a constant 5% of the H_2 .

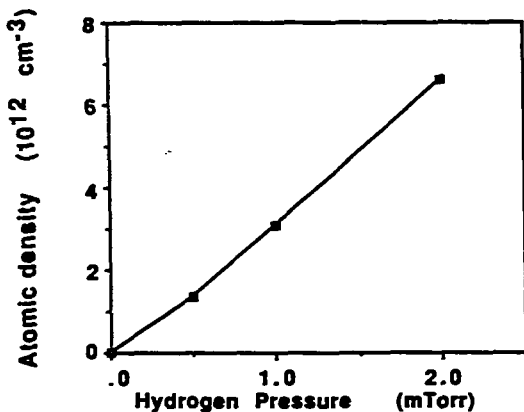


Figure 3. H^+ density as a function of H_2 pressure. Discharge conditions are 25A and 130V.

Figure 4 shows the results of a study conducted with varying discharge currents. Here the H_2 pressure was 20 mTorr and the discharge voltage was 90V. As can be seen, the H^+ density rises linearly with current over the range measured. However, the line does not extrapolate to $n_{H^+} = 0$ at $I_{\text{discharge}} = 0$. Figure 5 shows data obtained at lower H_2 pressure, 1 mTorr. Here, a definite nonlinearity in the H^+ density is observed.

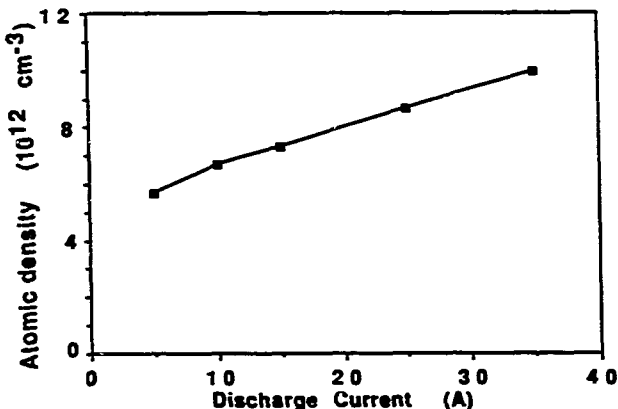


Figure 4. H^+ density as a function of discharge current. Discharge voltage is 90V and $p_{H_2} = 20$ mTorr.

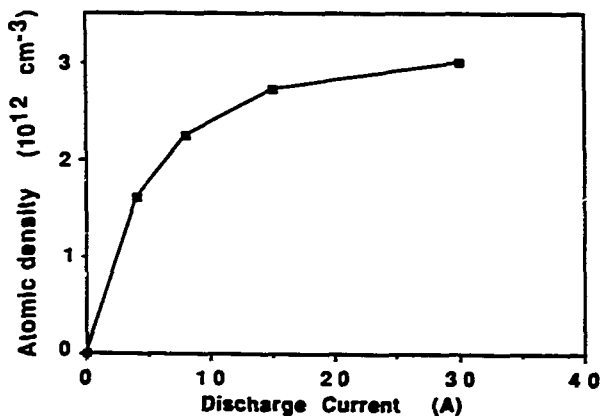


Figure 5. H^+ density as a function of discharge current, but at a lower H_2 pressure than Fig. 4. $p_{H_2} = 1$ mTorr, while discharge is at 100 V.

The populations of individual rotation-vibration levels of the H_2 in the discharge have been determined. For $v''=1$, (where the v'' refers to the vibrational level of the ground electronic state) the rotational distribution has been measured to $J''=13$. This data is shown in Figure 6. A thermal population distribution, when plotted as in Figure 6, would yield data points on a straight line. The slope of the line would then be inversely proportional to the rotational temperature, T_{rot} . As can be seen, this is not the case for our measurements. The first few J levels do lie on a line, however; using $J''=0$ to $J''=3$ yields $T_{rot} \sim 450K$. Obviously, the higher J level populations lie above the predicted values, showing that they are suprathermally populated.

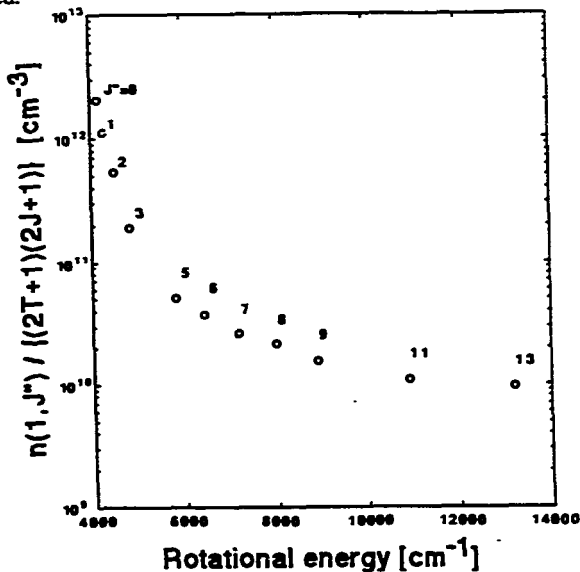


Figure 6. Rotational population distribution for $H_2(v''=1)$.

The dependence of the rotational distribution of $v''=1$ on changes in discharge conditions is illustrated in Figure 7. Note that over the range of conditions utilized, which include changes of factors of three in the discharge current and two in H_2 pressure, the rotational temperature is nearly constant at ~ 420 K. This indicates that the population in any particular J state is a constant fraction of the total population in any given v'' level. Because the fractional population in a J'' state is constant, the population in each v'' state can be determined by measuring the population in a single J state for each of the v'' levels.

Using this fact, the vibrational population distribution for this source is shown in Figure 8, where the $J''=1$ density is plotted for $v''=1$ through $v''=8$. In contrast to the rotational population distribution, the vibrational population distribution exhibits a Boltzmann distribution. The solid line represents a linear least square fit for $v''=1-8$ with $T_{vib} = 4150$ K.

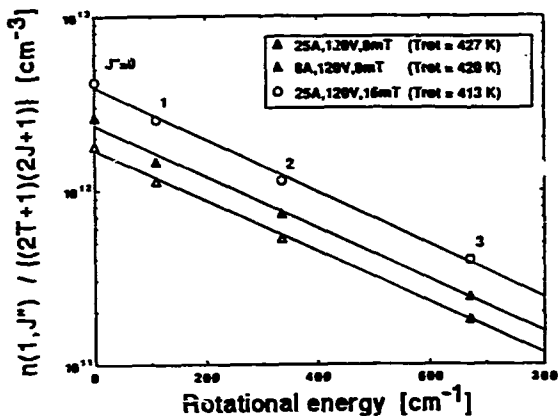


Figure 7. Rotational population of $J''=0-3$ for $H_2(v''=1)$ under various discharge conditions. Note the invariance of the rotational temperature.

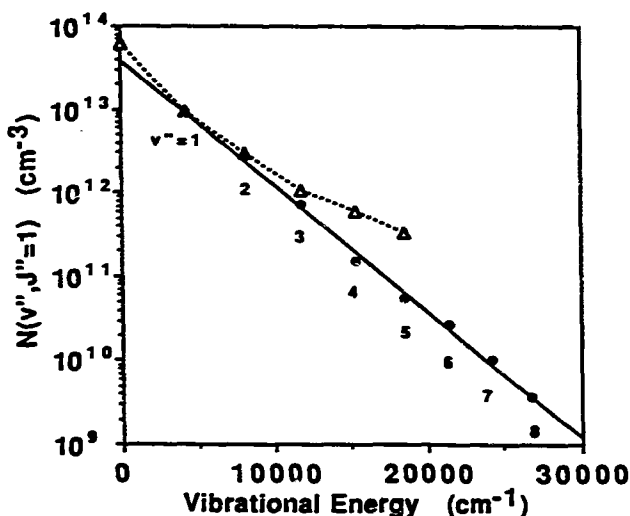


Figure 8. Vibration population distribution for volume source. The experimental points, the closed circles, were obtained at 25A, 120V and 8 mTorr H_2 . The solid line corresponds to a vibrational temperature of 4150 K. The triangles represent the calculated values of Hiskes, normalized to the experimental data at $v''=1$.

The dependence of four high-lying v'' , J'' states on discharge current is shown in Figure 9. Here, the population in $v''=4$, $J''=1$ and 3, and $v''=6$, $J''=1$ and 3 are shown with discharge currents from 2 to 25A. As can be seen, none of the states displays much variation in population over the range of the currents used. This shows that the rotational temperature of the low J'' states for these higher v'' states is relatively constant with discharge current, in agreement with the $v''=1$ data shown in Figure 6. It also demonstrates that the vibrational distribution up to $v''=6$ is insensitive to discharge current.

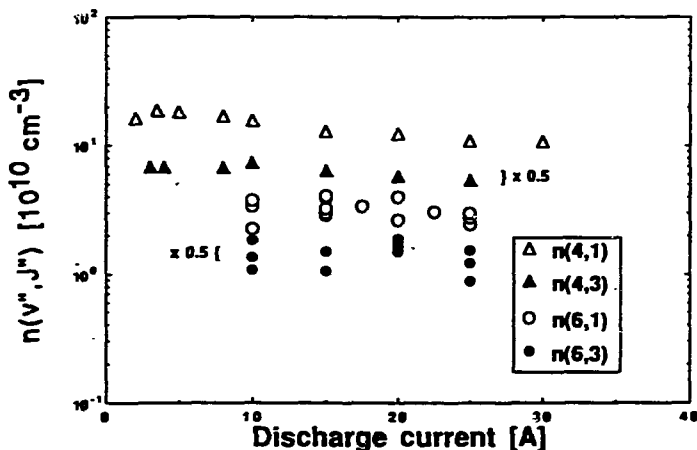


Figure 9. Dependence of the population of several high-lying v'' , J'' states on the discharge current. States measured are $v''=4$, $J''=1$ and 3, and $v''=6$, $J''=1$, and 3. Note the relative constancy of the populations.

DISCUSSION

The linear increase in H^+ density, as shown in Figure 4, is qualitatively as expected. That is, at modest discharge powers, more H^+ would be produced as the discharge current increases. At some point, however, one would expect the H^+ density to increase more slowly with discharge current. This is also observed, as seen in Figure 5. What is surprising is the modest dissociation fraction at which this slow increase occurs, ~5% for the conditions in Figure 5. Although the H_2 pressure for that data is only 1 mTorr, the nonlinear behavior illustrates the complicated kinetics taking place in these discharges.

The measured rotational-vibrational population distributions show that the H_2 is internally excited. The rotational levels above $J''=3$ are suprathermally populated, while those below can be characterized by a rotational temperature only slightly above room temperature. This can be explained if rotational relaxation processes occur on a

time scale which is short compared to vibrational relaxation. If this is the case, each vibrational level would rotationally equilibrate yielding a thermalized population distribution. The population in the high J'' states population may reflect the convolution of the nascent state distribution and the distribution of those H_2 which have only partially relaxed. Alternatively, the high J'' states may be the result of $V \rightarrow R$ energy transfer processes. More work is needed to resolve this question.

It is important to note that the rotational distributions for the low J'' levels of $v''=1, 4$ and 6 are very similar, as shown in Figures 7 and 9. This allows the determination of the various v'' populations to be made by measuring a single J'' state for each v'' level, as was done for Figure 8. This is particularly important for the higher v'' states as only one or two rotational levels could be observed in these sparsely populated levels. Changes in the rotational distribution for the higher v'' levels would cause inaccuracies in the vibrational population distribution; however, no variation in T_{rot} for v'' up to 6 was observed. In addition, because a large fraction of the population is in the state observed, $J''=1$, modest changes in the rotational temperature will not greatly affect the estimated vibrational distribution.

The vibrational distribution shown in Figure 8 exhibits a $T_{vib} = 4150$ K. Modeling of the source chemistry for these or similar discharge conditions has been performed by Hiskes and Karo⁵ and by Skinner, Bacal, et al.⁶ The dashed line in Figure 8 is the result of Hiskes for vibrational levels up to $v''=5$. The calculation and the measurement have been normalized at $v''=1$. As can be seen, the experiment and model disagree at higher v'' levels. The reason for the discrepancy is unknown. Although the Hiskes calculation used an electron density value 50% of the measured $1.6 \times 10^{12} \text{ cm}^{-3}$, increasing the electron density in the calculation would increase the vibrational population, giving a larger discrepancy. The model used by Skinner also overestimates the population in the higher v'' states, in spite of using the actual experimental electron density. The large population in $v'' \geq 6$ in an almost universal feature of models of H^- volume sources. This is the so-called "plateau" region, as the vibrational population distribution is predicted to flatten out for $v'' = 5-9$ for a number of calculations.^{7,8}

The only other *in situ* observation of $H_2(v'')$ within the discharge is by Pealar et al.⁹ who used Coherent Antistokes Raman Scattering to observe a high pressure multicusp discharge. That experiment observed $v'' \leq 3$. The only other experiment to observe the higher v'' states is by Eenshuistra et al.,¹⁰ who detected states with $v'' \leq 5$ effusing from a multicusp source using a multiphoton ionization technique. Under some conditions, this group observed a non-thermal distribution, with a plateau starting to appear at $v''=4$. As discussed above, the results presented here, which include data at higher v'' , show no evidence for a plateau. At this time it is not possible to determine if the divergent results are due to different source physics or experimental technique.

The prevailing theory of H^- production in volume sources invokes the mechanism of dissociative attachment of low energy electrons to vibrationally excited molecules. This theory requires the presence of H_2 with $v'' \geq 6$ in relatively large amounts, and is reflected in the models of these sources by the previously discussed plateau. The measurements reported here, the first observations of $v'' > 5$, exhibit a thermal vibrational distribution out to $v''=8$, the present sensitivity limit of the technique. It must be pointed out that this source has not been optimized for H^- production, and the H^- density within the plasma has not been measured. However, the size, shape, and plasma parameters of this discharge chamber are similar to those of optimized tandem multicusp sources, with the exception that the present source does not have a magnetic filter. Instead, additional strong cusp fields are used to increase the plasma confinement. It was anticipated that the plasma processes in this

source would be similar to those in the driver region of tandem volume sources. This has not yet been verified, but if true, the formation mechanism of H^- in volume sources may need to be re-evaluated.

CONCLUSIONS

Recent results using VUV laser absorption spectroscopy to probe the physics of H^- volume sources have been reviewed. The ability to measure quantitatively H^- and $H_2(v^*)$ *in situ* in a plasma has been demonstrated. Measurement of H^- and $H_2(v^*)$ have been obtained for a variety of discharge conditions. In particular, rotational-vibrational state distributions have been obtained for vibrational states up to $v''=8$. These measurements, in contrast to model predictions, show a thermalized vibrational distribution, with $T_{vib} \sim 4200K$.

ACKNOWLEDGEMENTS

The work presented represents the contributions of many colleagues. These include A.S. Schlachter, J.W. Stearns, G.T. Worth, B. D'Etat, and H.F. Döbele. This work has been supported by the Air Force Office of Scientific Research, Los Alamos National Laboratory, and the Director, Office of Energy Research, Office of Fusion Energy, Development and Technology Division, of the U.S. Department of Energy under contract No. DE-AC03-76SF00098.

REFERENCES

1. G.C. Stutzin, A.T. Young, A.S. Schlachter, J.W. Stearns, K.N. Leung, W.B. Kunkel, G.T. Worth, and R.R. Stevens, *Rev. Sci. Instrum.* **59**, 120 (1988).
2. G.C. Stutzin, A.T. Young, A.S. Schlachter, J.W. Stearns, K.N. Leung, W.B. Kunkel, G.T. Worth, and R.R. Stevens, *Rev. Sci. Instrum.* **59**, 1479 (1988).
3. G.C. Stutzin, A.T. Young, A.S. Schlachter, K.N. Leung, and W.B. Kunkel, *Chem. Phys. Lett.* **155**, 475 (1989).
4. G.C. Stutzin, A.T. Young, H.F. Döbele, A.S. Schlachter, K.N. Leung, and W.B. Kunkel, *Rev. Sci. Instrum.*, in press.
5. J.R. Hiskes and A.M. Karo, *Appl. Phys. Lett.* **54**, 508 (1989).
6. D.A. Skinner and M. Bacal, private communication, and D.A. Skinner, P. Berlemont, and M. Bacal, these proceedings.
7. J.R. Hiskes, A.M. Karo, and P.A. Wilmann, *J. Appl. Phys.* **58**, 1759 (1985).
8. C. Gorse, M. Capitelli, M. Bacal, and J. Bretague, *Chem. Phys.* **117**, 177 (1987).
9. M. Pealot, J.-P.E. Taran, M. Bacal, and A.M. Bruneteau, *J. Chem. Phys.* **82**, 4943 (1985).
10. P.J. Eenshuistra, R.M.A. Heeren, A.W. Kleyn, and H.J. Hopman, *Phys. Rev. A* **40**, 3613 (1989).